academicJournals

Vol. 10(1), pp. 1-13, 15 January, 2015
DOI: 10.5897/SRE2014.6061
Article Number:E5C391D49532
ISSN 1992-2248

http://www.academicjournals.org/SRE

Scientific Research and Essays

Full Length Research Paper

Coastal climate and beach dynamics at Ponta do Ouro, Mozambique

Mark R. Jury[1,2]

[1]Geography Department, University of Zululand, 3886 South Africa.
[2]Physics Department, University of Puerto Rico Mayaguez, 00681 USA.

Received 2 August, 2014; Accepted 10 December, 2014

Annual field surveys conducted at Ponta do Ouro in Southern Mozambique have determined that coastal variability is driven by high wave energy and consequent northward longshore drift. There is a log-spiral headland-bay system marked by 80 m tall forested dunes in the south that give way to a broad flat sandy beach. Marine climate processes that affect coastal erosion and accretion are studied using local and remote data sets. Since surveys began, the climate has undergone a prolonged dry spell (2002-2007) followed by increased run-off and easterly winds (2010-2013) that have re-built the beaches. Sand grain sizes vary from 240 - 410 μm (coarser south – finer north) and are mobilized by frequent longshore wind events > 10 m/s. Ocean drifters reveal a northward current in the outer surf zone of 0.6 m/s and an onshore gyre of 0.1 m/s in the recessed bay. Wave-driven sand transport is estimated at 5 10^6 kg/yr/m. While the upper beach has flattened due to pedestrian traffic and urban development, the lower beach has recovered from erosion due to a greater frequency of easterly waves and rainy weather.

Key words: Beach, coastal erosion, marine climate.

INTRODUCTION

Geological history, wave characteristics, tidal range and littoral drift are responsible for shaping coastlines and associated hazards such as instability, erosion and inundation (Kaliraj et al., 2013). The bathymetry and shelf slope influence sediment deposition (Trenhaile, 1997; Ridderinkhof et al., 2000), while the concentration of suspended sediment is related to wave energy, depth of surf zone and longshore wave-driven currents (Christie and Dyer, 1998); and can be monitored by satellite imagery (Bassoullet et al., 2000; Lee et al., 2004). Wave propagation over a narrow shelf results in high energy on the coastline and greater mobilization of sediment (Carter et al., 1990; Frihy and Lotfy, 1997; Lacey and Peck, 1998; Manson et al., 2005). Changes in the width of beach dunes can be traced to natural forces and human activities that deplete coastal vegetation, particularly compaction at access points (Maktav et al., 2002). Seasonal to multi-annual variations in wave energy produce cycles of shoreline erosion and accretion (Wright and Short, 1984; Chauhan et al., 1996; Benumof et al., 2000; Georgiou and Schindler, 2009; Saravanan et al., 2011; Smith et al., 2014). Rapid changes happen with

E-mail: mark.jury@upr.edu

storm surges and tourism development (Chandrasekar et al., 2000; VanRijn 2009).

Log-spiral bays are found on many of the world's wave-dominated coastlines (Carter, 1988). They consist of an up-coast headland with a hook shape and a down-coast open bay, whose processes transition from dissipative to reflective beach stages associated with coarser grain size and steepening slope. Silvester (1984) found that the log-spiral shape depends on the prevailing oblique wave energy and distance between headlands. Large log-spiral bays like Algoa on the south coast of Africa have wave-driven longshore transport of 1 m/s on the headland and 0.1 m/s in the leeward bay under prevailing westerly winds (Goschen and Schumann, 2011) that induce longshore sand transport of 3×10^5 m^3/yr. Sediment suspended by breaker turbulence is pushed along by the current, in conjunction with bedload transport. Sand also moves on the beach face by swash and wind, accounting for ~15% of the total (Silvester and Hsu, 1993).

Sandy beaches backed by elevated dunes are a prominent feature of the coastline between South Africa and Mozambique 26-27.5°S and 32-33.5°E. Coastal sediments are mobilized by wave-driven longshore currents on the outer edge of the surf zone. Sediment available for reworking into coastal landforms is derived from previous geological fluctuations and shelf deposits. Variations in sea level have left a system of inland lakes and wetlands behind a line of recently formed sand dunes. Small rivers drain into these wetlands, so the main source of coastal sediment is from distant South African rivers such as the Umfolozi and Tugela. Northward near-shore currents cast these sediments toward Mozambique. The warm Agulhas current ensures coral reef growth, tropical fisheries and comfortable air and sea temperatures ~ 25°C. Yet the weather is changeable due to marine storms which pass at regular intervals even in summer (Tinley, 1985). The lower beach experiences a tidal range of ~ 1.8 m and wave action from the southeast (Figure 1a). Sand bars line the coast < 100 m offshore and create breaker zones linked by rip currents.

The warm eastern seaboard incubates a great diversity of marine and terrestrial life. About 10 million people live within 10 km of the coast from Maputo to Durban and there has been a coastward shift in economic production over the past 30 years. Coastal tourism plays a growing role (⅓) in Mozambique's $15 B economy. The coastal zone is urbanizing so an understanding of its dynamic nature is essential for effective management under rising sea levels (~0.17 cm/yr). Our focus here is on Ponta do Ouro at the Southern border of Mozambique where a prominent headland diverts the winter waves. The town was deserted in the 1975-1990 civil war, but has since recovered with the advent of coastal tourism. People flock to the beaches for recreation and diving on the coral reefs (~ 100 000 times/yr), bringing economic benefits and environmental consequences (Bjerner and Johansson, 2001; Perry, 2001; Jury et al., 2011b).

Our study region is exposed to passing storms from the Indian Ocean and Mozambique Channel. There are no weather stations or oceanographic moorings, so a variety of secondary datasets are used to describe regional conditions, supplemented by *in-situ* field data collected as part of a long-term coastal monitoring project. One aim of this work is to support sustainable development through generation of knowledge on the coastal dynamics; specifically to study the apparent cycle of coastal erosion and accretion and its relation to changes in coastal weather and storm-induced waves.

Background

Ponta do Ouro is located at 26.84°S and 32.89°E (Figure 1a, 4a) atop low sand dunes with an easterly view of the Indian Ocean. The area of the town is ~ 10 km^2, situated 120 km south of the capital city of Maputo. The sandy soils drain quickly and have little organic content for crop production (Table 1b). The southern coastal dunes have gradients near 35%, while the town is relatively flat. The vegetation is sub-humid savannah comprised of dry coastal forests that transition abruptly to prairie grasslands. The farming capacity is limited by low soil moisture; consequently most food is imported.

Until 2000 the natural landscape was conserved except for cropping around the wetlands and some deforestation for fuel-wood collection (Faria and Sitoi, 1996). Residential developments have since spread over the grassland near the point. There are no rivers in Ponta do Ouro only two small lakes ~ 2 km inland. Currently there is no water distribution system; water is drawn from wells of reasonable quality. In pre-war surveys there were over 5000 species of animals recorded in Southern Mozambique (Faria and Sitoi, 1996). The biodiversity has largely recovered since the civil war, despite a dysfunctional municipality. Ponta do Ouro's population has grown from 1600 in 2005 to 3000 by 2014, with rural development spreading inland and tourism along the coast.

Ponta do Ouro extends prominently ~ 1 km seaward as a narrow band of 80 m forested sand dunes in the south that give way to 10 m sparsely covered dunes in the recessed bay. Sheets of sand penetrate the dune forest on the south side of the headland, and are continually re-vegetated. The warm waters, tropical fishery and coral reefs attract divers (Bjerner and Johansson, 2001) and tourism resorts have proliferated in the leeward bay.

DATAS AND METHODS

Annual field surveys have been made since year 2000 to understand the coastal dynamics and resource use via photographs, opinion polls and objective data collection. Low-tide beach profiles have been surveyed by theodolite in the bay next to the headland and at the hotel further north, so that evolving beach profiles can be tracked. Google digital-earth scenes over the past

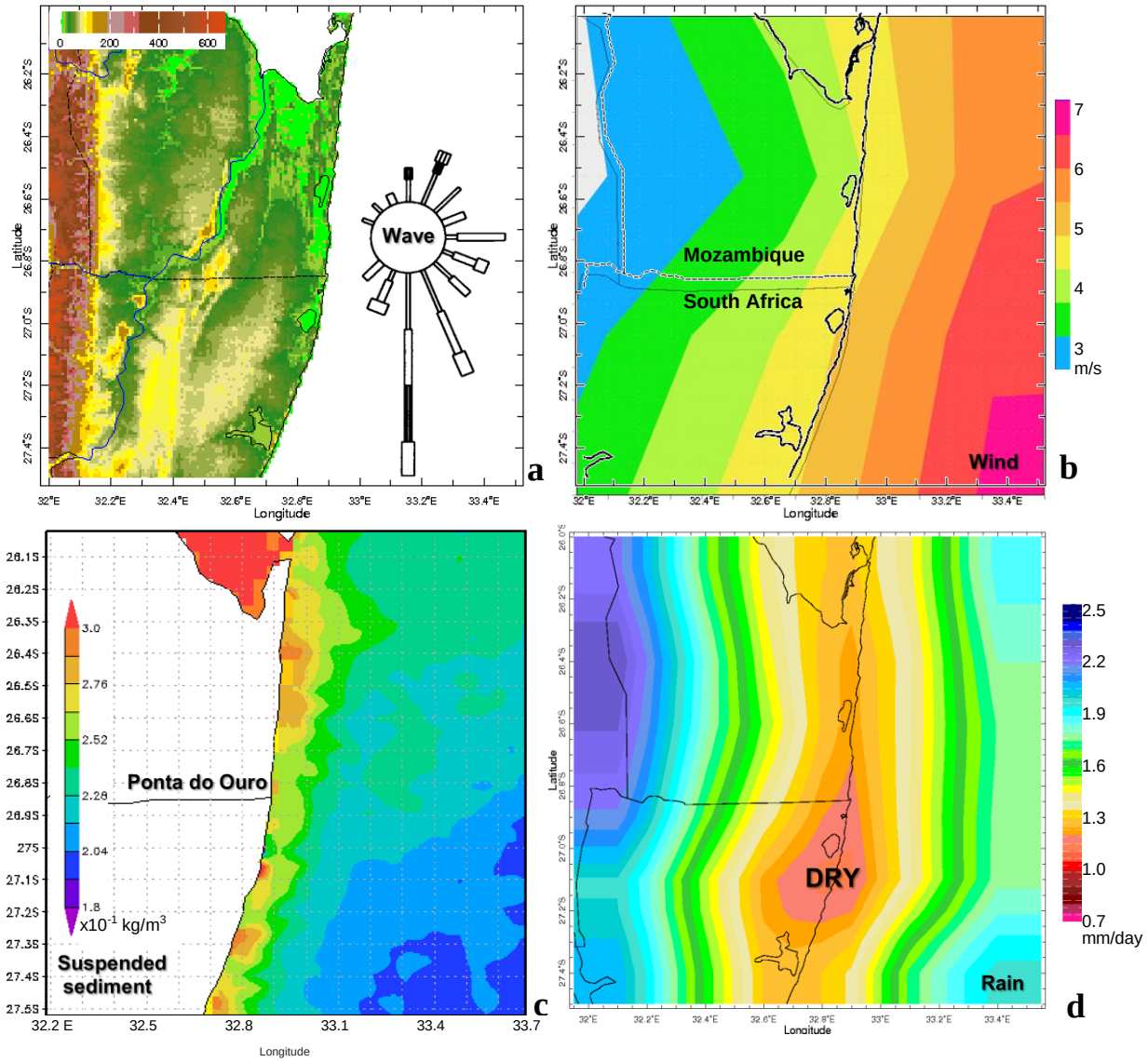

Figure 1. (a) Topography. 2000-2013 averages of (b) CFS wind speed, (c) NASA satellite suspended sediment, (d) cMorph satellite rainfall. Inset in (a) is ocean wave direction (from) and height rose at 5% (length) and 1 m (thickness) intervals. Refer to Figure 6 for large-scale context.

decade were viewed to delineate the beach edge. Sand samples of ~ 200 g were collected twice on the lower beach and foredune. Samples were dried and sieved at ranges from 1000 to 50 μm and grain size distribution was analyzed. Nutrient analysis was done to determine the proportion of P, Ca, K, Mg, pH, NO_3, C, cat-ions and moisture available. Littoral zone currents were monitored using a drifting drogue launched in the surf and tracked at one minute intervals using two theodolites on the foredune. Drifter tracking was repeated on many occasions in different seasons and frequency histograms were calculated. Local wind patterns were observed during two surveys and composite vectors were calculated for prevailing directions: 1. onshore, 2. southerly and 3. northerly. Continuous monthly discharge of the Umfolozi River 185 km to the south was obtained from the South African Dept of Water Affairs website.

Apart from *in-situ* surveys, regional characteristics (26-27.5°S and 32-33.5°E) were analyzed at 5 km resolution from NASA satellite derived surface temperature, rainfall (Joyce et al., 2004) and marine suspended sediment (or water clarity, euphotic depth). Spatial maps were averaged over the years 2000-2013 and monthly time series were extracted for the grid point at Ponta do Ouro. Coastal weather was analyzed for surface wind and moisture via Coupled Forecast System (CFS) model reanalyses at 20 km resolution (Saha et al., 2010). Wave generation was studied using histograms of daily CFS marine wind data sorted for easterly (-U) and southerly (+V) gales, and the associated composite weather maps were plotted. Ocean wave data were analyzed from the South African Data Centre for Oceanography ship database for a grid point off Ponta do Ouro, and from European Community (ECMWF) model reanalysis per direction sector, as height - period histograms (Sterl and Cairns, 2005). Ocean reanalysis mean maps and frequency histograms were calculated using the 8 km hybrid

Table 1. Beach sand / soil characteristics (a) south of Ponta and (b) inland from the point.

(a)	Mabibi Dune	Kosi Dune	Kosi Shore
Density	1.46	1.41	1.31
P	2	8	5
K	0	0	110
Ca	115	115	75
Mg	120	100	280
cat-ions	1.56	1.40	2.96
pH	9.48	9.08	9.23
(b)	**Grassland**	**Forest**	**Wetland**
P	11	38	10
K	308	361	347
NO3	4	17.5	15
% C	0.77	2.37	0.45
% moist	0.70	3.32	1.32

coordinate ocean model (Chassignet et al., 2009) based on Navy coupled data assimilation (since 2005). Long-term sea surface height trends were analyzed from the nearest gauges together with ship-based sea surface temperature anomalies. The results are given in sequence from regional- to micro-scale; some figures are called out of order to maintain the flow of discussion.

RESULTS

Marine climate pattern and trend

Figure 1a to d summarizes the coastal climate. The topography consists of a 70 km plain of lowlands < 100 m elevation. The coastline near the border is slightly convex and thus exposed to the marine weather. The wind speed pattern (Figure 1b) is dominated by a strong gradient formed by high speeds (7 m/s) offshore and low speeds (3 m/s) inland. Marine suspended sediment is relatively low (Figure 1c), but there is a coastal strip ~10 km wide with values up to 0.3 kg/m^3 that pass northward with wave-driven currents. The satellite rainfall map (Figure 1d) reveals a marked dry zone < 1 mm/day that extends along the coast north and south of Ponta does Ouro. Further inland and offshore rainfall increases to 2.5 mm/day. The low rainfall relates to accelerated winds over the convex coastline.

Mean maps and histograms from the Hycom 8 km ocean reanalysis are analyzed in Figure 2. The frequency distribution of daily longshore currents is Gaussian with a 45% occurrence of northward flow, and median near zero (Figure 2a). Southward currents are equally likely outside the surf-zone. The mixed layer depth near the coast averages ~20 m, and its histogram has an inverted Gaussian distribution with many shallow and deep cases due to calm and stormy weather (Figure 2b). The mean map of temperature reveals a 15 km wide coastal strip of 24°C water; values increase offshore to 25°C (Figure 2c). Mixed layer depths (Figure 2d) are greatest in the 10-50 km coastal margin, reflecting stronger winds there. Meridional currents at the coast are weak (Figure 2e) and there is a coastward reduction in onshore flow (Figure 2f) that characterizes the land-sea interface. The onshore flow traps sediment in a narrow coastal corridor, as seen in Figure 1c.

Monthly time series since 2000 are given in Figure 3a-c. The water budget from CFS reanalysis (Figure 3a) indicates that 2000 year was wet, but 2002-2005 were dry with little run-off. Soil moisture remained near 200 mm (10%) from 2002 until 2010. Thereafter, many rainy spells induced greater soil moisture, run-off and Umfolozi River discharge in Jan 2011 and Oct 2012 - Jan 2013. This put increased sediment into the coastal zone. Spectral analysis of Umfolozi discharge anomalies back to 1948 (not shown) indicates cycling at 2-4 and 11 years, consistent with Corbello and Stretch (2012b).

Satellite estimated land and sea temperatures (Figure 3b) exhibited regular annual cycling. Land temperatures rose quickly in early summer, while sea temperatures peaked in late summer. The seasonal amplitude exceeded inter-annual variance in the period of study (2000-2013). The marine euphotic depth or seawater clarity varied from 100 m in summer to 50 m in winter (Figure 3b) as storm generated waves and associated near-shore currents stir the sand. Of all the variables reviewed, land surface temperature is best correlated with euphotic depth ($r = +.67$ for $N=168$), indicating that warm weather is associated with clear water.

Winds and waves

Surface winds (Figure 3c) are plotted for offshore and inland points. The U time series exhibits a strong coast to inland gradient, and was most negative (onshore from

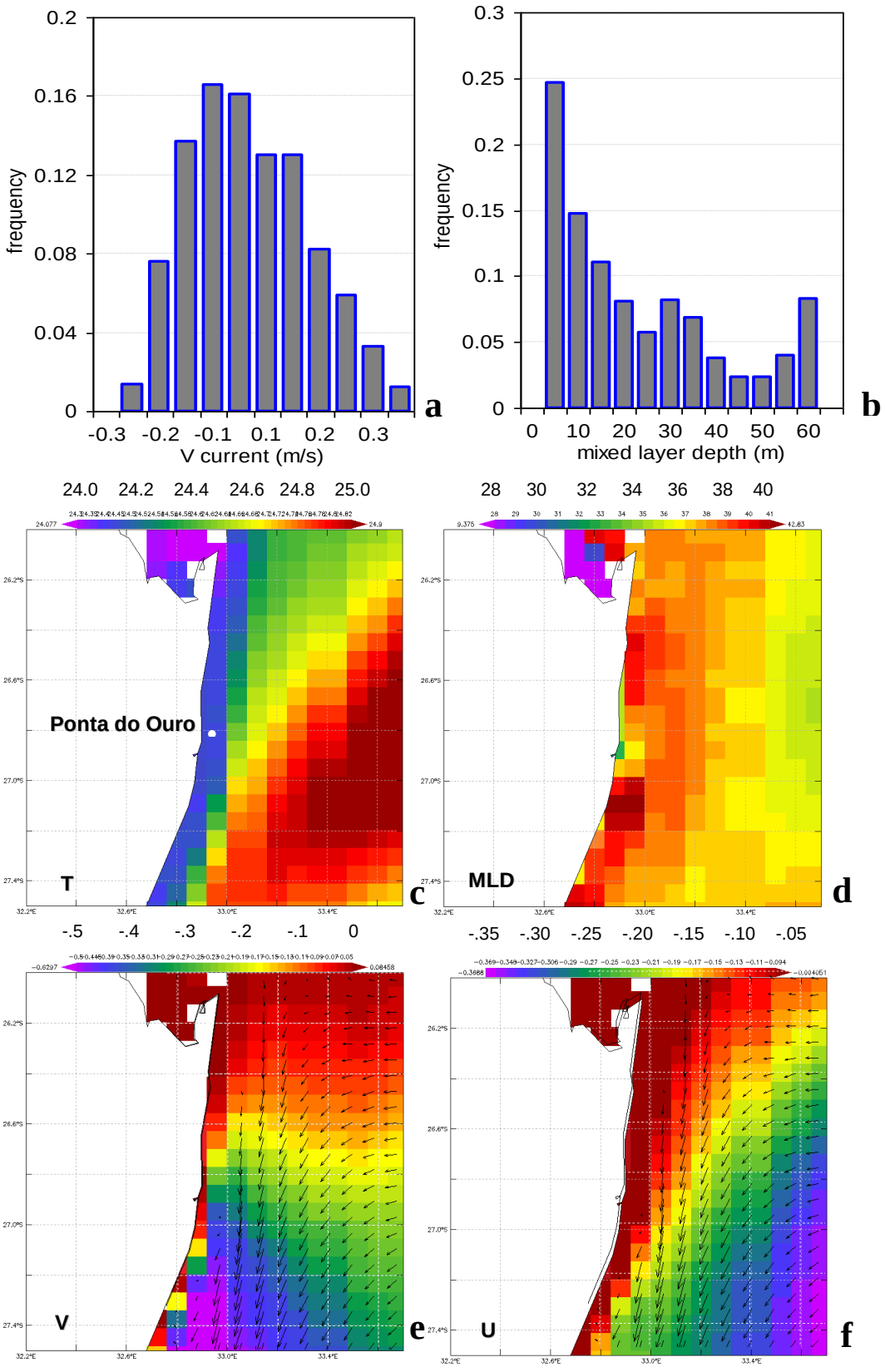

Figure 2. Frequency histogram of coastal (a) V current and (b) mixed layer depth based on daily Hycom data at Ponto do Ouro: point in (c). Mean ocean maps from 8 km Hycom reanalysis of: (c) temperature, (d) mixed layer depth, (e,f) V and U currents (shaded and vectors).

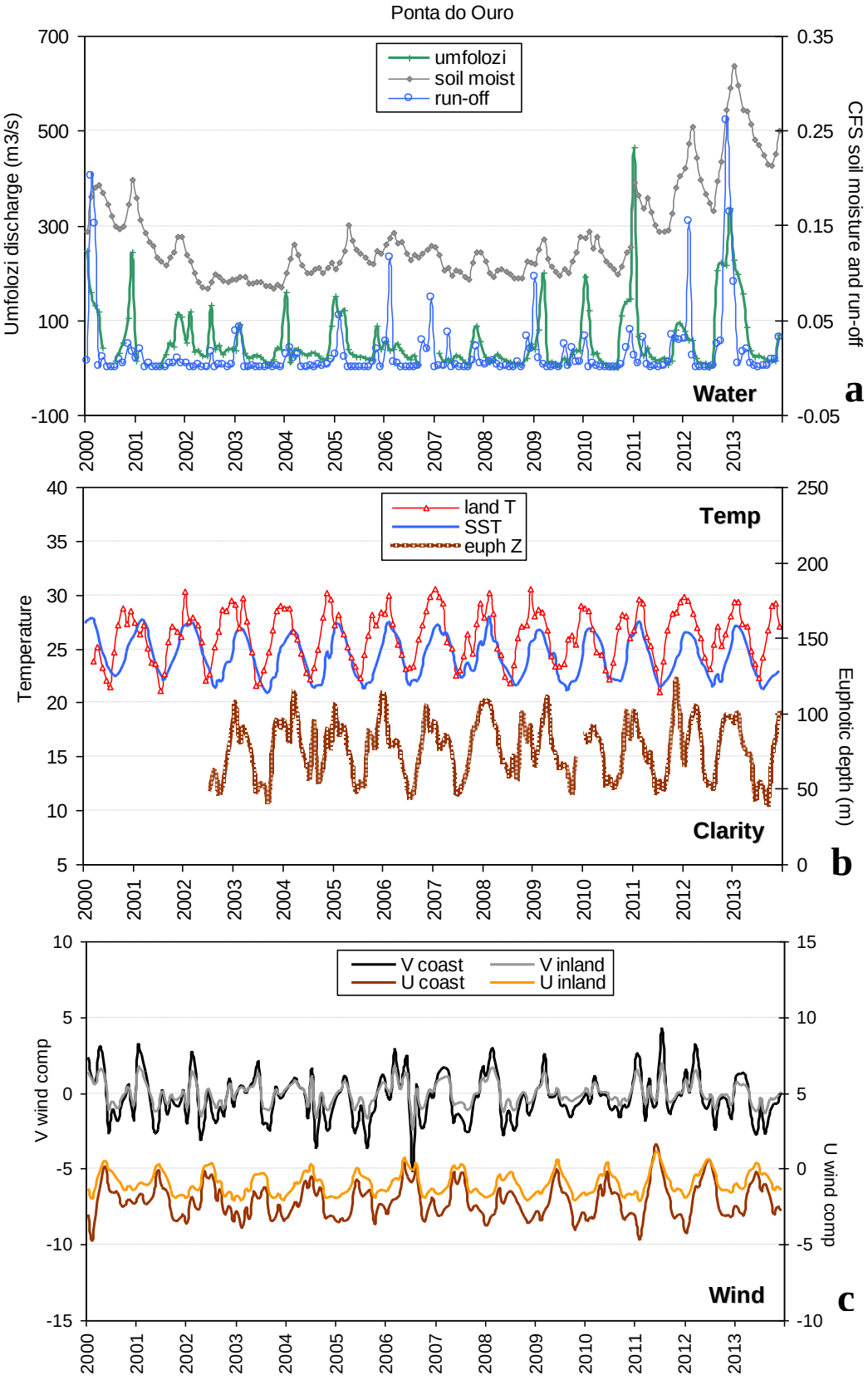

Figure 3. Ponta do Ouro monthly time series of (a) CFS soil moisture (mm/2 m) and run-off (mm/day) and Umfolozi discharge (M m^3/s), (b) NASA satellite daytime land surface and sea temperature (C) and marine euphotic depth (m). (c) CFS wind components (U, V, m/s, at offshore and onshore points).

Table 2. Number of days per 3 year period with wave-generating storm winds > 10 m/s lasting > 3 days averaged over a 15 x15° area southeast of Ponta.

Years	±2001	±2004	±2007	±2010	±2013
From east	26	17	22	41	46
From south	20	27	33	30	22

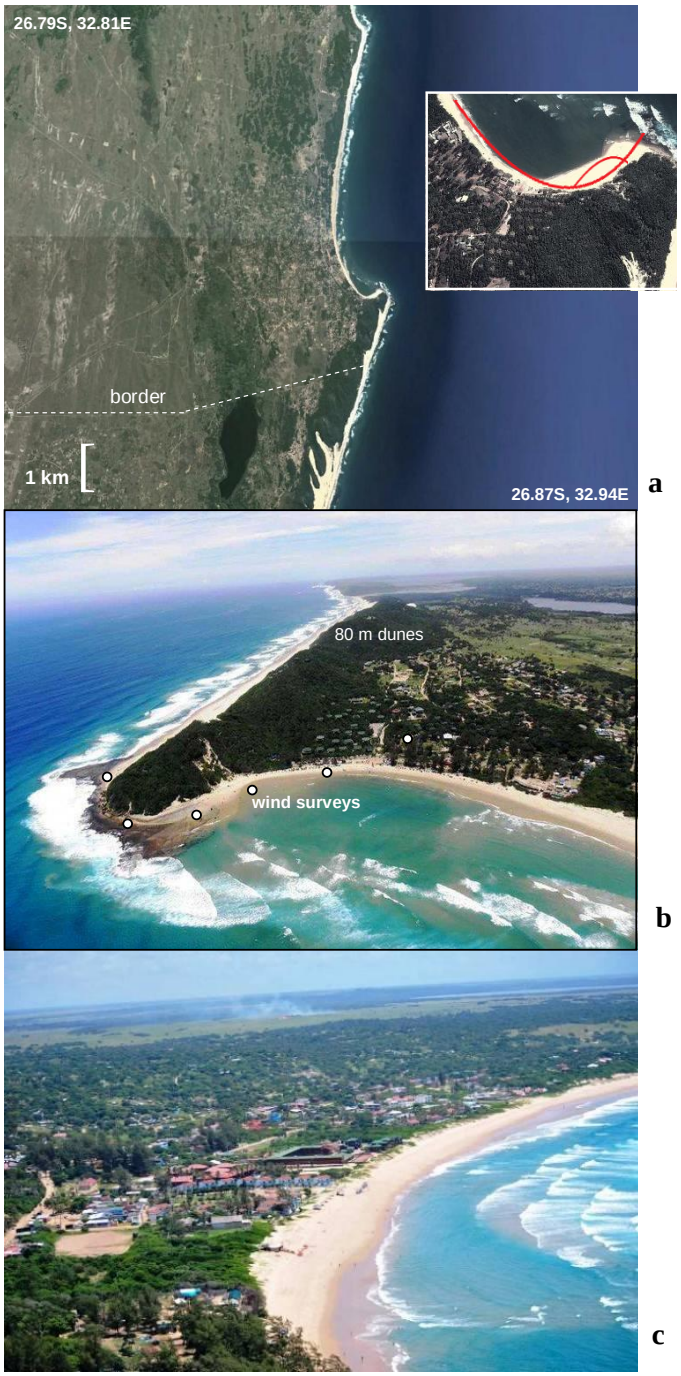

Figure 4. (a) Digital-earth composite photo of Ponta do Ouro 2013 and bay inset with 2005 shoreline and 2010 cusp (red lines). (b) Aerial photos of the point viewed toward south, (c) and bay toward north.

east) during summer, particularly in 2011 and 2012. It is argued that spells of onshore wind produce short period waves that accumulate sand deposits in the recessed bay. Periods of strong southerly wind (+V) are irregular and spike during sequences of mid-latitude storms. These coincide with large swells and strong northward currents that tend to remove sand from the beaches. Because storm-induced waves affect the sediment budget, a histogram analysis of daily –U and +V winds in the 'fetch' area 24-38°S and 32-42°E was made in three year intervals (Table 2). Cases of southerly winds > 10 m/s vary from 20 in 2001 to a peak of 33 in 2007 and decline back to 22 days by 2013. However, cases of easterly winds > 10 m/s show an increase from 17 in 2004 to 46 days in 2013. Easterly waves (and northerly winds) tend to limit the longshore export of sand. Thus losses in the 2004-2007 period reversed since 2010 (Figure 4a, 7a) and coincide with a wetter climate (Figure 3a). Easterly swells are generated in summer when tropical troughs and mid-latitude anticyclones pass south of Madagascar. The composite wind pattern for peak days: 5 Jan 2011, 11 Dec 2011, 27 Mar 2013 illustrates this weather scenario (Figure 6a) consistent with local winds in Figure 6d. On the other hand, southerly swells derive from winter mid-latitude cyclones, whose weather scenario for peak days: 2 Jul 2005, 25 Jun 2006, 28 Jun 2009 shown in Figure 6b generates strong local winds that converge leeward of the headland (Figure 6e).

ECMWF wave climate histograms are analyzed for the three directions (Figure 6a to c). ESE waves are characterized by 1-3 m height and 5-6 s period, SSW waves are of longer period and greater height, while NNE waves are of short period (4-5 s). Each wave regime generates different coastal responses. The short period waves from NNE and ESE dampen the longshore currents, trapping sediment and building the beaches. But long period waves from the SSW have a deeper reach and put sand in suspension for northward export. Wave production is constrained by Madagascar to the northeast, eastward storm movement and minimal heat flux except during southerly winds (Figure 6c).

The north-easterly scenario offers a wind-blown dimension. Wind speeds > 10 m/s capable of mobilising sand of ~ 300 μm grain size (Kaczmarek et al. 2005) are NNE 15% of the time, mostly in spring: 27 Sep 2012, 29 Aug 2013 and 19 Sep 2013. Local winds are channeled and accelerate around the headland. There is an inland gradient of wind ~ 1 m/s per 100 m owing to friction of the headland compared with the adjacent sea. During

Figure 5. Photos at Ponta do Ouro of (a) Wind blown dunes outside the point in 2013 (at S), (b) headland reef at low tide 2007 (at E), (c) leeward bay beach 2003, (d) receded beach and flattened dunes 2013 (at N in Figure 8a).

easterly directions (Figure 6a,d) the flow splits and winds decline at the coast, aiding sand deposition.

Coastal dynamics

Sand samples from Ponta do Ouro have grain sizes in the range 240 - 410 μm. Coarser sediments are found south of the point, finer sediments are seen in the recessed bay (Figure 7b). Wave-induced longshore drift (Figure 8a) creates a sandbar northwest of the point which acts as a sediment bypass and creates a fine wave for recreational surfing. The seaward excursion of the current across the headland leaves an onshore gyre in the recessed bay, where beach and dune sedimentation are de-coupled (Psuty, 1992). Further north the beach widens and coastal dunes grow (Figure 4c).

Offshore coral reefs are too deep to cause refraction or dissipation of wave energy around Ponta do Ouro, so back-beach berms and cliffed foredunes are common. Concave sections of dune face, exposed headland reef, chunks of sandstone rock on the beach (Figure 5b), and beach profiles (Figure 7a) give evidence of coastal recession and recovery from 2005 to 2013 depending on the marine climate (Table 2).

Sediment budget

Littoral transport processes are dependent on wave climate and sediment characteristics (Miller, 1999). These data are available from climatological sources and project information (Figure 3a to c, 7b). The wave climate in summer-winter consists of 140-170° direction, 1.6-1.9 m height, and 6.5-7.8 s period. Ocean swells > 4 m occur ~ 10% of the time and correspond with cyclonic storms (Corbello and Stretch, 2012a). Surf zone currents then reach 1 m/s, whereas during anticyclonic intervals the currents subside. The mean wave energy is calculated as $E = \int_{Þ}(H^2\ T \sin ɵ)$, integrated over frequency distribution (Þ), where H is wave height, T is wave period, and ɵ is the diffracted wave angle (~30°). A value of 9 kW/m is calculated at Ponta. Like many southern hemisphere locations, high wave energy is maintained throughout the year. About 85% of longshore sediment transport takes place in the shallow surf zone (Aijaz and Treloar, 2003).

Littoral transport is estimated as in VanWellen et al. (2000) and Esteves et al. (2009): $Q_s = \int_Z(V*C)$, where V is the longshore current and C is sediment concentration (~ 0.3 kg/m^3 ± 0.1). Drifter results at Ponta indicate V ~ 0.6 m/s ± 0.2 (Figure 8a), similar to the theoretical longshore current (Kaliraj et al., 2013): $V = 20(s)(gH)^{0.5}\sin ɵ$, where s is slope (3 10^{-2}), H is diffracted wave height (~1 m) and ɵ ~30°. From these inputs, it is estimated that ~ 5 10^6 kg/yr/m is transported northward in the surf zone, values slightly above Ganesh and Gopaul (2013) for a log-spiral bay in Trinidad. On the bay-side beaches, volume fluctuations of ~ 10 m^3/yr are noted (Figure 7a) due to

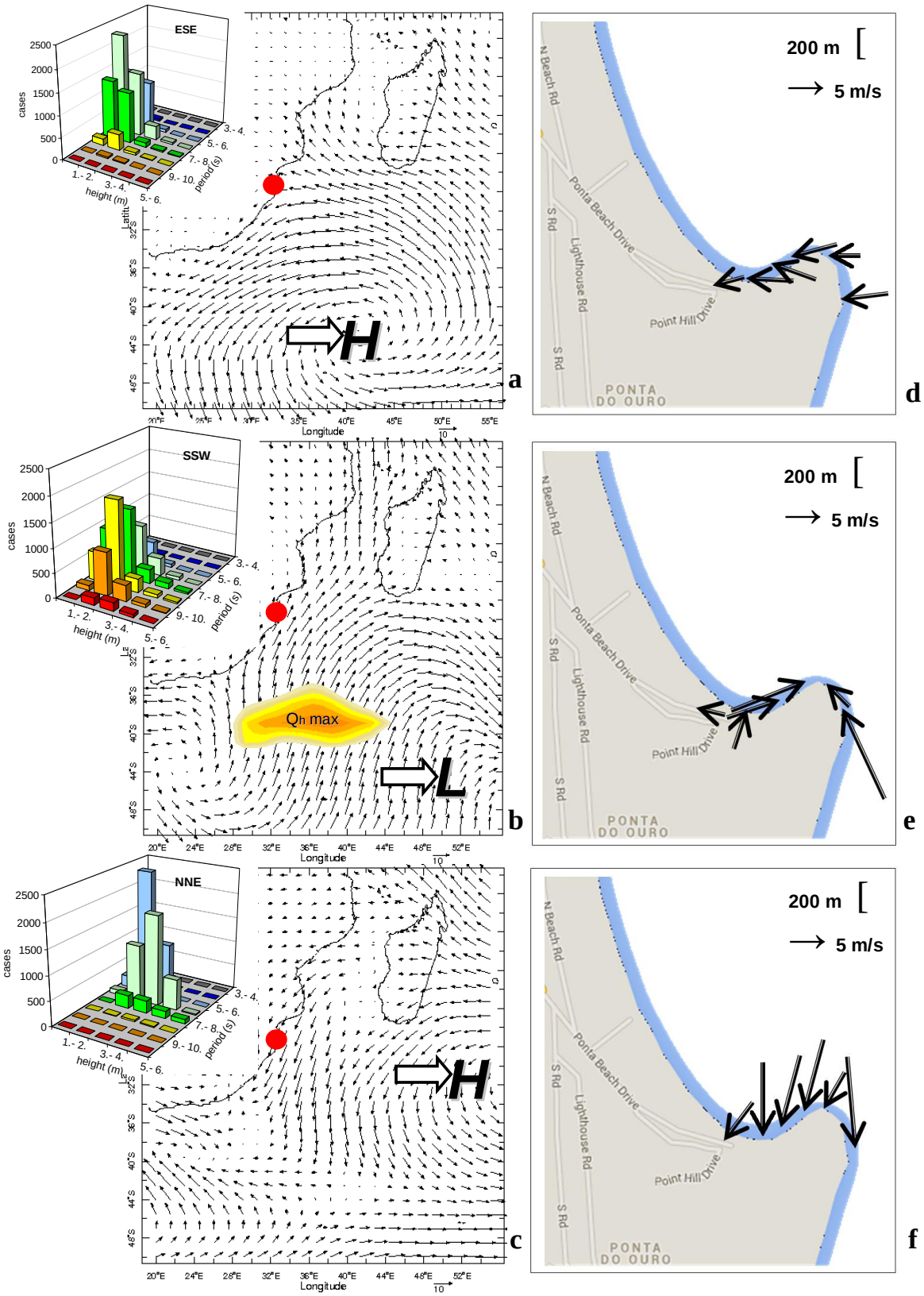

Figure 6. Regional composite patterns of: (a) East wave scenario in late summer; (e) South wave scenario in winter with region of turbulent flux > 150 W/m^2 shaded yellow; (c) North wind scenario in spring. Block arrows denote pattern translation. (d-f) Corresponding observed local winds with length scale. Inset on left are ECMWF wave climatology histograms per direction. Red dot is Ponta do Ouro.

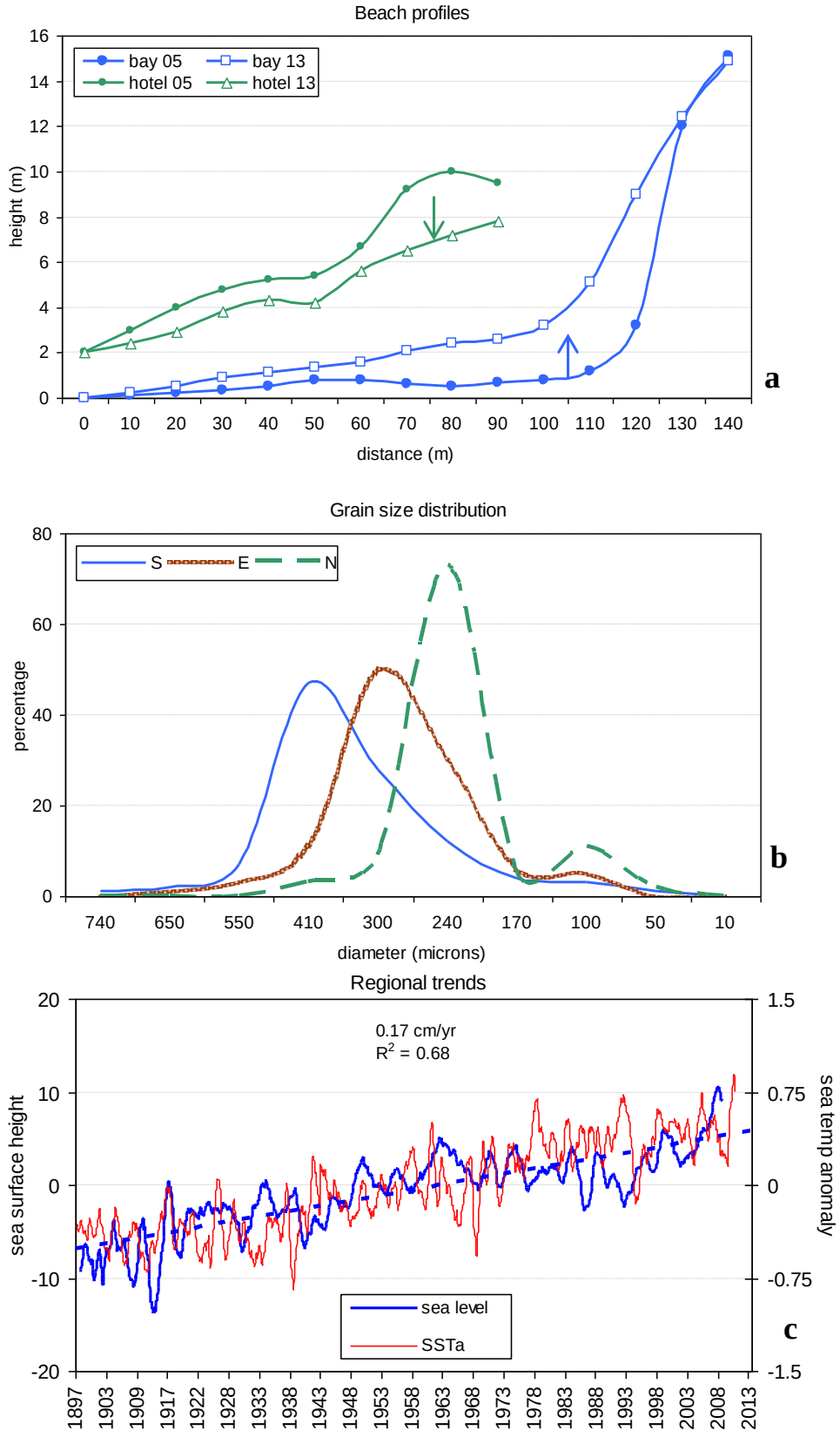

Figure 7. Beach profiles at hotel and bay in 2005 and 2013; hotel offset by +2 m. (b) Sand grain size distribution for samples taken on the north, east and south side of the headland (sites in Figure 8a). (c) Century long record of regional sea surface height and trend (cm), and local sea temperature anomaly.

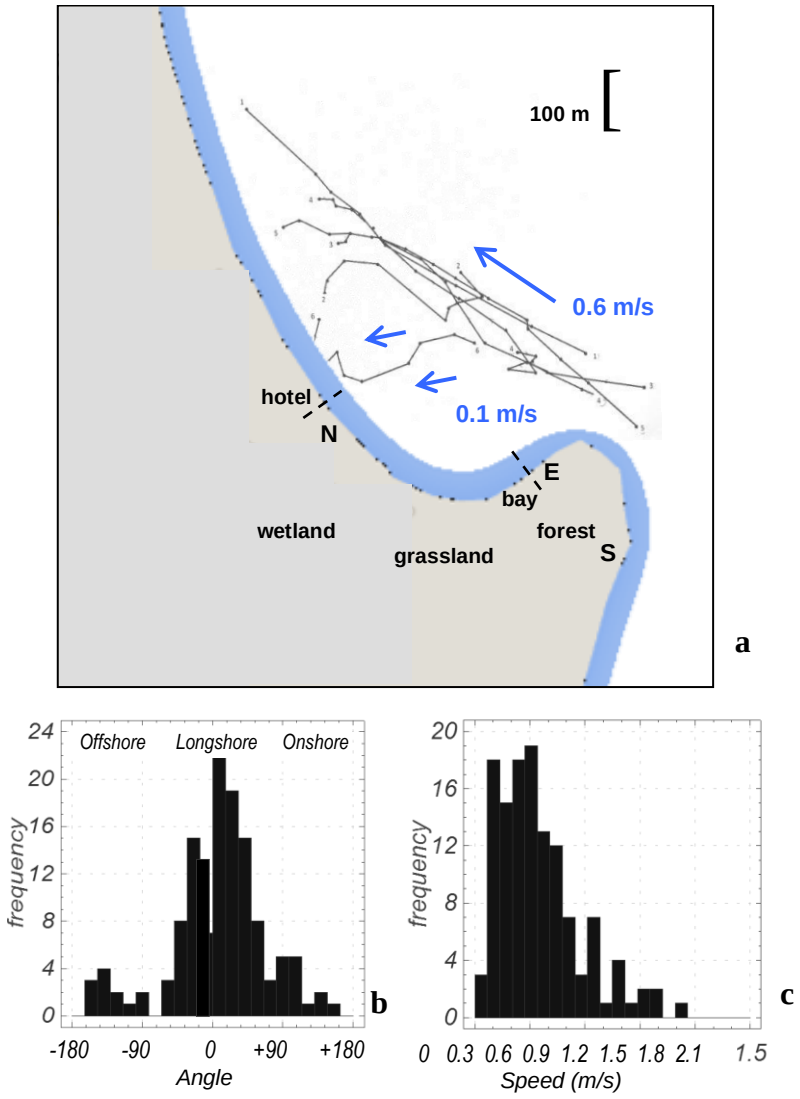

Figure 8. (a) Drifter tracks 23-25 April 2002, with vectors representing mean values in surf and bay zones. Frequency distribution of all drifter tracks: (b) direction and (c) speed. Labels in (a) refer to sites of sand and soil samples, and beach profiles (dashed).

sand bypass and human activities. On-going surveys in 2013 found the lower beach had regained mass while the upper beach had flattened (Figure 7a).

SUMMARY

Coastal dunes are mobile features, yet town planners and managers often view the beach as static. The headland at Ponta extends < 1 km seaward and shelters a bay from wave action and northward drift. Our results show that easterly waves which favour accretion increased from 2011-2013. Southerly waves which favour erosion, were most frequent around 2005. Northerly winds suppress longshore currents and build the dunes. The natural quasi-decadal cycle of beach erosion and accretion is amplified because dry spells coincide with southerly waves, while wet spells (river sediment) coincide with easterly waves. These assertions require data analysis over another decade to understand wave - sediment relationships in the context of storm events.

There is on-going human pressure on marine resources despite the partial recovery of tidal fauna after beach driving was banned in 2003. Ponta do Ouro is the only town on this coast that supports waterfront housing and tourist facilities. Development there is at risk of beach recession from inadequate planning and storm surges. Offshore waters are warming (+.01C/yr) and sea levels are rising (Figure 7c) so impacts are on-going. A pedestrian boardwalk along the foredune is recommended

to limit erosion. The management of eco-tourism development should be guided by scientific insights and serviced by local government, to sustain this beautiful and dynamic coast.

ACKNOWLEDGEMENTS

UNESCO initially sponsored the long-term monitoring project in Coast and Small Islands. Mr G. Mulder of University of Zululand is thanked for collecting and calculating drifter tracks and beach profiles. Earlier work by J. Mitchell and A. Mthembu University of Zululand assisted this study. Remote data were analyzed from NASA-giovanni, IRI-climate library, Climate Explorer-knmi, Univ. Hawaii-adprc, Google-Earth and SA Dept Water Affairs websites.

Conflict of Interest

The authors have not declared any conflict of interest.

REFERENCES

Aijaz S, Treloar D (2003). Beach management options at Botany Bay Australia, Proc. Oceans 2003 symposium, San Diego, USA.

Bassoullet P, Hir PL, Gouleau D, Robert S (2000). Sediment transport over an intertidal mudflat: field investigations and estimation of fluxes within the Baie de Marennes-Oleron (France). Cont. Shelf Res. 20:1635-1653.

Benumof BT, Storlazzi CD, Seymour RJ, Griggs GB (2000). The relationship between incident wave energy and seacliff erosion rates: San Diego County, California. J. Coast Res. 16:162-1172.

Bjerner M, Johansson J (2001). Economic and environmental impacts of Nnture based tourism: A case study of Ponta do Ouro, Mozambique, Univ Edwardo Mondlane Technical Report.

Carter RWG (1988). Coastal Environments: An Introduction to the Physical, Ecological and Cultural Systems of Coastlines. Academic Press, London UK, pp. 213-217.

Carter RWG, Jennings SC, Orford JD (1990). Headland erosion by waves. J. Coast Res. 6:517-529.

Chandrasekar N, Anil C, Rajamanickam M, Rajamanickam GV (2000). Coastal landform mapping between Tuticorin and Vaippar using IRS-1C data. Indian J. Geomorphol. 5:114-120.

Chassignet EP, Hurlburt HE, Metzger EJ, Smedstad OM, Cummings JA, Halliwell GR, Bleck R, Baraille R, Wallcraft AJ, Lozano C, Tolman HL, Srinivasan A, Hankin S, Cornillon P, Weisberg R, Barth A, He R, Werner F, Wilkin J (2009). US GODAE: Global ocean prediction with the Hybrid coordinate ocean model (Hycom). Oceanography 22:64-75.

Chauhan P, Nayak S, Ramesh R, Krishnamoorthy R, Ramachandran S (1996) Remote sensing of suspended sediments along the Tamil Nadu coastal waters. J. Ind. Soc. Remote Sens 24:105-114.

Christie MC, Dyer KR (1998). Measurements of the turbid tidal edge over the Skeffling mudflats. in: Black KS, et al. (eds) Sedimentary processes in the intertidal zone. Geol. Soc. London Spec. Publ. 139:45-55.

Corbello S, Stretch DD (2012a). The wave climate on the KwaZulu-Natal coast of South Africa. J. South Afr. Instit. Civ. Eng. 54:45-54.

Corbello S, Stretch DD (2012b). Decadal trends in beach morphology on the east coast of South Africa and likely causative factors, Nat. Hazards Earth Syst. Sci. 12:2515-2527.

Esteves LS, Williams JJ, Lisniowski MA (2009). Measuring and modelling longshore sediment transport, Estu. Coast. Shelf Sci. 83:47-59.

Faria M, Almedia S (1996). Plano de Desenvolvimento e Gestão dos Recursos Naturais do Distrito de Matutíne, Maputo.

Frihy OE, Lotfy MF (1997). Shoreline changes and beach-sand sorting along the northern Sinai coast of Egypt. Geo-Mar Lett. 17:140-146.

Ganesh R, Gopaul N (2013). A Predictive Outlook of Coastal Erosion on a Log-Spiral Bay (Trinidad) by Wave and Sediment Transport Modelling, in: Conley, D.C., et al. (eds.), Proc 12th Intl Coastal Symp (Plymouth), J. Coastal Res. 65:488-493.

Georgiou IY, Schindler JK (2009). Wave forecasting and longshore sediment transport gradients along a transgressive barrier island: Chandeleur Islands, Louisiana. Geo-Mar Lett. 29:467-476.

Goschen WS, Schumann EH (2011). The physical oceanographic processes of Algoa Bay, SAEON-IMT report, P0106-110000-730002.

Joyce RJ, Janowiak JE, Arkin PA, Xie PP (2004). CMORPH: A method that produces global precipitation estimates from passive microwave and infrared data at high spatial and temporal resolution. J. Hydrometeorol. 5:487-503.

Jury MR, Cuamba P, Rubuluza P (2011b). Development strategies for a coastal resort in southern Mozambique. Afr. J. Bus. Manage. 5(2):481-504.

Kaczmarek LM, Ostrowski R, Pruszak Z, Rozynski G (2005) Selected problems of sediment transport and morphodynamics of a multi-bar nearshore zone. Estu. Coast. Shelf Sci. 62:415-425.

Kaliraj S, Chandrasekar N, Magesh NS (2013). Impacts of wave energy and littoral currents on shoreline erosion/accretion along the south-west coast of Kanyakumari, Tamil Nadu using DSAS geospatial technology. Environ Earth Sci. doi10.1007/ s12665-013-2845-6.

Lacey EM, Peck JA (1998). Long-term beach profile variations along the south shore of Rhode Island, USA. J. Coast Res. 14:1255-1264.

Lee HJ, Jo HR, Chu YS, Bahk KS (2004) Sediment transport on macrotidal flats in Garolim Bay, west coast of Korea: significance of wind waves and asymmetry of tidal currents. Cont. Shelf Res. 24:821-832.

Maktav D, Erbek FS, Kabdasli S (2002). Monitoring coastal erosion at the black sea coasts in turkey using satellite data: A case study at the lake Terkos, north-west Istanbul. Int. J. Remote Sens. 23:4115-4124.

Manson GK, Solomon SM, Forbes DL, Atkinson DE, Craymer M (2005). Spatial variability of factors influencing coastal change in the Western Canadian Arctic. Geo-Mar Lett. 25:138-145.

Miller HC (1999). Field measurements of longshore sediment transport during storms, Coastal Eng. 36:301-321.

Perry C (2003). Reef Development at Inhaca Island, Mozambique. Ambio 32:134-139.

Psuty N (1992). Spatial variation in coastal foredune development, in R. Carter, et al. (ed.), Coastal Dunes: Geomorphology, Ecology and Management for Conservation. Hague, Balkema, pp. 3-13.

Ridderinkhof H, van der Hama R, van der Lee W (2000). Temporal variations in concentration and transport of suspended sediments in a channel-flat system in the Ems-Dollard estuary. Cont. Shelf Res. 20:1479-1493.

Saha S, Saha S, Shrinivas M, Hua-Lu P, Xingren W, Jiande W, Sudhir N, Patrick T, Robert K, John W, David B, Haixia L, Diane S, Robert G, George G, Jun W, Yu-Tai H, Hui-Ya C, Hann-Ming HJ, Joe S, Mark I, Russ T, Daryl K, Paul Van D, Dennis K, John D, Michael E, Jesse M, Helin W, Rongqian Y, Stephen L, Huug Van Den D, Arun K, Wanqiu W, Craig L, Muthuvel C, Yan X, Boyin H, Jae-Kyung S, Wesley E, Roger L, Pingping X, Mingyue C, Shuntai Z, Wayne H, Cheng-Zhi Z, Quanhua L, Yong C, Yong H, Lidia C, Richard WR, Glenn R, Mitch G (2010). The NCEP Climate Forecast System Reanalysis. Bull. Am. Meteor. Soc. 91:1015-1057.

Saravanan S, Chandrasekar N, Sheik Mujabar P, Hentry C (2011). An overview of beach morphodynamic classification along the beaches between Ovari and Kanyakumari, Southern Tamil Nadu coast, India. Phys. Oceanogr. 21:130-141.

Silvester R (1984). Ecological effects of various coastal defence systems. J. Water Science & Technology, 16(3-4):355-365.

Silvester R, Hsu JRC (1993). Coastal Stabilization. Prentice Hall, NJ. 578 p.

Smith AM, Guastella LA, Botes ZA, Bundy SC and Mather AA (2014). Forecasting cyclic coastal erosion on a multi-annual to multi-decadal scale: Southeast African coast, Estu. Coast. Shelf Sci., doi10.1016/j.ecss.2013.12.010.

Sterl A, Caires S (2005). Climatology, variability and extrema of ocean waves - The Web-based KNMI/ERA-40 Wave Atlas. Int. J. Climatol. 25:963-977.
Tinley K (1985). Coastal dunes of Southern Africa, Foundation for Research and Development, South Africa.
Trenhaile AS (1997). Coastal dynamics and landforms. Clarendon, Oxford, 366 pages.
VanRijn LC (2009). Prediction of dune erosion due to storms, Coastal Eng. 56:441-457.
VanWellen E, Chadwick AJ, Mason T (2000). A review and assessment of longshore sediment transport equations for coarse-grained beaches. Coastal Eng. 40:243-275.
Wright LD, Short AD (1984) Morphodynamic variability of surf zones and beaches: A synthesis. Marine Geol. 50:93-118.